Published by
NIGERIAN SOCIETY OF PHYSICAL SCIENCES
Available online @ https://journal.nsps.org.ng/index.php/jnsps

J. Nig. Soc. Phys. Sci. 7 (2025) 2270

Journal of the Nigerian Society of Physical Sciences

Variation, distribution and trends of aerosol optical properties in Africa during 2000-2022

Aladodo Sarafadeen Shehu[a,*], Ibrahim Bolaji Balogun[b], Ibrahim Yakubu Tudunwada[a]

[a]*NASRDA, Centre for Atmospheric Research, Anyigba, Nigeria*
[b]*Department of Science Laboratory Technology (Physics/Electronics), Kwara State Polytechnique, Nigeria*

Abstract

Global anthropogenic emissions have been on the increase causing environmental and climatic concerns. To this end, aerosol properties influenced by these anthropogenic activities from satellites (MODIS, OMI, and AIRS) and ground remote sensing (AERONET) data were examined for distribution, variation, and trends over Africa during 2000–2022. Furthermore, the response of temperature to the interaction of aerosols with solar radiation was investigated in the region to reflect the aerosol impact on the regional climate and serving as an indicator for climate change. The spatial distribution of the aerosol properties were characterized as high (Aerosol Optical Depth, AOD ≥ 0.5, Angstrom Exponent, AE ≥ 0.7, Absorption Aerosol Optical Depth, AAOD ≥ 0.1, and Single Scattering Albedo, SSA ≥ 0.95), moderate (AOD $\equiv 0.3$, AE $\equiv 0.5$, AAOD $\equiv 0.08$, and SSA $\equiv 0.9$), and low values (AOD ≤ 0.2, AE ≤ 0.2, AAOD ≤ 0.05, and SSA ≤ 0.85) which varied with time and local emissions dependence. In addition, trends in AOD show a significant decrease in the arid areas of the northern and southern regions, while an increase in the arid Sahel and central Africa. AE is on a decreasing trend as well as AAOD, except for the southern central Africa, which has a significant positive trend of AAOD attributed to intense bush burning. A dust hotspot in the central Sahara and central South Africa smoke experienced positive and neutral trends in SSA respectively indicating an increase in scattering aerosol (pure dust) and a uniform level of smoke emission in the areas, with other areas negatively trending. A strong positive relationship exists between air temperature a popular climate change indicator with AOD, AAOD, and SSA and negative ones with AE based on the level of aerosol composition and types. The study forms the basis for establishing aerosol climate change indicator in Africa a region of high aerosol load.

DOI:10.46481/jnsps.2025.2270

Keywords: Aerosol properties, Trend, AOD, Climate

Article History :
Received: 25 July 2024
Received in revised form: 05 October 2024
Accepted for publication: 14 October 2024
Available online: 22 March 2025

Communicated by: Oladiran Johnson Abimbola

1. Introduction

The rise in average temperature of the Earth's near-surface air over the past century has received much attention related to global climate change, like precipitation, which varies more than temperature on spatial and temporal scales over a region [1]. Research has shown that precipitation microphysics is largely affected by the particulate matter in the atmosphere (aerosol) as well as other climatic variables [2, 3]. The environment, transportation, and human health are other areas at the receiving end of aerosol in what are classified as direct and indirect aerosol effects. Chemically, major tropospheric

*Corresponding author: Tel. No.: +234-806-264-3948.
Email address: aladodoshehu@gmail.com (Aladodo Sarafadeen Shehu)

aerosol species are: sulphate, black and organic (brown) carbon, dust, and sea salt [4–6]. Rapid industrialization and urbanisation, along with fossil fuel consumption and bush burning in the last two decades, have substantially increased globally the anthropogenic aerosol components over their natural sources and have become a major environmental and climatic concern. In addition, aerosols have a considerable contribution to climate change uncertainties [7]. Thus, determining the long-term trend and variation of aerosol optical and absorption properties and the underlying causes in a region of high aerosol producers and emitters, such as Africa, is beneficial to understanding regional climate variability and air quality conditions. Africa is the world's largest source of dust and smoke [8, 9]. Dust steaming out of Africa towards the Atlantic Ocean and the Mediterranean Sea is emitted from various localised sources in the arid and semi-arid areas of the Sahara and Sahel, differing in intensity, seasonality, and frequency. Likewise, the smoke emanating from Sub-Sahel and southern African regions due to bush and agricultural burning as well as firewood cooking due to the high cost of LPG in recent times.

The parameters of aerosols considered in this work, namely aerosol optical depth (AOD), absorption aerosol optical depth (AAOD), angstrom exponent (AE), and single scattering albedo (SSA) represent important characteristics of aerosols that can be used to analyse climate change. AOD represents the vertical column aerosol load in the atmosphere; AAOD is the amount of the absorbing component of the aerosol load; AE is for the particle size of the aerosols; and SSA represents the light absorption characteristic of the aerosol. These key properties of aerosol population loading play a major role in determining the magnitude of radiation forcing in terms of scattering and absorption of incoming solar radiation and cloud formation, thus having a high climate impact. Using the Maxwell theory, the Lambert-Beer law can be derived which describes how the light beam is reduced due to extinction by particles as shown in equation (1).

$$\frac{dI(\lambda)}{dz} = -b_{ext} I_0(\lambda), \tag{1}$$

where I_0 and I are intensities of the incoming and exiting radiation respectively while b_{ext} is the aerosol extinction coefficient m^{-1}. Integrating equation (1) gives the quantity of transmitted light through aerosol layer of height z resulting to AOD [10].

$$I(\lambda) = I_0(\lambda) e^{(-\int_0^z \alpha_{aer}(\lambda,\ z)dz)}, AOD = \int_0^z \alpha_{aer} dz, \tag{2}$$

where z is the path of the light from the Sun through the atmosphere. AE described the relationship of the AOD as function of the wavelength of light in addition to the aerosol size distribution which can be derived from two optical depths at two different wavelengths as shown in equation (3).

$$AE = \frac{\log(AOD_{\lambda 1}/AOD_{\lambda 2})}{log(\lambda_1/\lambda_2)}, \tag{3}$$

where λ is the wavelength [11]. SSA is the fraction of light extinction to that of scattered which is represented mathematically as;

$$SSA = \frac{\sigma_s}{(\sigma_s + \sigma_a)}, \tag{4}$$

where σ_s is the light scattering coefficient and σ_a is the light absorption coefficient. The implication of these aerosol properties to climate change study are numerous and directly involved [12].

Some climate change indicators (CI) have been developed to diagnose and track changes in observable climate system properties through time [13, 14]. The CIs were used to track changes in the physical, chemical, and anthropogenic components of the climate system. Their spatial and temporal resolutions are on either a regional or global scale. Some CI focus on the drivers of global change, while others are more strongly focused on response variables. Examples of CIs include regional and global air temperature, precipitation, sea level, sea and land ice, and atmospheric concentrations of carbon dioxide, methane, nitrogen oxides, and fluorinated gases. Meanwhile, very few CIs of climate-relevant to aerosol properties were developed on a regional or global scale [15] based on lack of extensive data record. Like other CIs, aerosol-CIs can be used to quantify variability and temporal trends in aerosol populations in the atmosphere and changes attributable to drivers of aerosol variability such as primary aerosol emissions, gaseous precursor, and meteorological conditions.

Seasonal aerosol variation from year to year over the African continent is being linked to the movement of intertropical discontinuity (ITD) coupled with trade winds from north and south, different major and minor local aerosol sources (dust in Sahara, Sahel, and smoke from south), atmospheric dynamics, shifting air-masses, and minor contributions from long transport routes as well as meteorological conditions [15–18]. Several studies conducted at a regional and global scale have utilised remote sensing satellite data or ground-based remote sensing instruments and sometimes both, with models for comprehensive monitoring of the long-term behaviour and dynamics of the atmospheric aerosol. Khamala *et al.* [19] study the long-term climatology and spatial trends of aerosol optical depth over east-Africa from 2001 to 2019 using the MODIS and MERRA-2 datasets. An increase in AOD that was positive and significant was shown by the spatial trend analysis conducted over the arid and semi-arid parts of the study area, which changes with seasons.

Long-term aerosol optical properties variation and characteristic study were conducted over Hong Kong combining both AERONET and satellite observations from 2006 to 2021 by Yu *et al.* [20]. This shows seasonality in the variation of the properties, with lower AOD but higher AE, and SSA in summer, and elevated AOD but lower AE and SSA in spring and winter. Zhang *et al.* [21] implemented non-linear trend analysis on global AOD using ensemble empirical mode decomposition (EEMD), which gives the perception of providing more perceptible changes than linear trends. A study of the trend in the aerosol characteristic over the Indo-Gangetic and North China plains reveals a rising trend of fine-mode particulate AOD over

the study area [22]. Other studies in different African sub-regions over the long-term have observed a significant increasing trend of aerosol in populated urban areas while remote and serene areas experienced a decreasing trend, which is associated with high anthropogenic emissions in the cities as a result of being densely populated and decreasing natural sources of aerosol, respectively [23–26]. Also, seasonal variability in aerosol composition, Load, types, and sources has being reported in sub-regional studies [6, 27–29].

Most previous studies of aerosol variation and trend conducted due to its role in radiation budget, cloud formation, air quality, and climate in the African region concentrated mainly on variation and trend in AOD, whereas long-term changes in AAOD, AE, and SSA are barely in focus as considered in this study. In addition, only satellites remote sensing data, which are prone to cloud cover, single time passage and retrieval biases leading to over- or underestimation of parameters, were utilised in the studies. Also, to the best of our knowledge, no previous studies from the region have considered the whole African region in a study with all the parameters stated couple with the fact that the region presents very low active AERONET stations compared to other developed regions of the world. This study utilises the ground-based remote sensing AERONET database version 3 level 2.0, which is cloud cleared temporal data over ten different locations in the region from north to south and adjourning islands with 10+ years of data, complemented with satellite measurements of MODIS and OMI for effective regional coverage and representation. The study period starts at the beginning of the twenty-first century (2000), when African states economies started to emerge and contribute significantly to the global anthropogenic aerosol level. The combination of the two observation methods in this study gives a detailed and holistic view of the aerosol in the African region and serve as foundation for establishing aerosol climate change indicator in the region in addition to the role it play in radiation budget and air quality.

2. Geographic and meteorology of the study area

Africa is made up of 54+ countries and five sub-regions bounded by latitudes 35°N to 35°S of the equator and longitudes 20°W to 50°E of the Greenwich Meridian, including neighbouring islands. It is bathed by two oceans, the Atlantic to the west and the Indian Ocean to the east; two seas, the Mediterranean to the north and the Red Sea to the north-east; and tens of major rivers across the board (Figure 1). Africa has the world's largest desert, the Sahara, which lies in North and West Africa, the largest dust aerosol source and the Kalahari desert in the South [30]. It has different seasons in the year categorised into four (DJF, MAM, JJA, and SON), and the vegetation varies based on the geographical location of each country. The wind system over Africa has different forms, power, and direction depending on the sub-region, altitude, and physical phenomena that form it. Based on Köppen's climate classification, The African climate is arid in the north and part of the south-west, tropical around the equator, which cuts across the west, the central and upper parts of the south, and temperate in the south-east. Tropical and arid zones are relatively dominated by the movement of the Inter-Tropical Convergence Zone (ITCZ) and the associated Hadley circulation [31]. High levels of precipitation are associated with the deep clouds at the ITCZ, and the precipitation pattern changes between the summer and winter, therefore, producing the African 'wet' and 'dry' seasons [32]. The Hadley circulation brings about different trade winds in the north during the dry season, such as north-easterly (Harmattan) trade winds over the Sahara. During the wet season, North Africa is subject to more intense convection due to the more northerly location of the ITCZ and more intense solar radiation. Further north, over the Sahara, this is dominated by dry convection, whereas further south, this convection will become moister and associated with more precipitation. The geographic information of the ten (10) AERONET sites selected for the study are as shown in Table 1. Tamanrasset site situated at the highest altitude of 1377 m (m. s. l.) good for capturing long range transported aerosol and Cape Verde site is at the lowest altitude of 60 m.

3. Instrumentation and dataset

3.1. AERONET

It is a worldwide network of scanning Sun radiometers for aerosol observation at nine spectral channels from 340 to 1640 nm, providing high-accuracy data output during daytime after being cloud screened and manually inspected [33, 34]. AERONET Version 3 Level 2.0 is the cloud cleared, quality-assured with pre- and post-field calibration data recently released by the NASA Godard Space Flight Centre (https://aeronet.gsfc.nasa.gov), which is adopted in this study. A detailed descriptions of the instrumentation, calibration, data processing, data quality, *almucantar* retrieval, and inversion algorithm are described elsewhere [35–38]. Ten AERONET sites spread across Africa with more than ten years of data (2000–2022) were selected for the study, catering for different aerosol sources, transport routes, types of areas such as the city, remote areas, islands, desert areas, forest areas, and semi-desert, [6] as well as climates (arid, tropical, and temperate). The AERONET sites are Saada and Cairo, representing the farthest North Africa; Tamanrasset, for the central Sahara; Cape Verde, for the island; Banizoubou, Cinzana and Zinder, for the Sahel; Ilorin, for the sub-Sahel; Mongu and Skukuza, for Southern Africa (Figure 1). The AOD and AE at 440 and 440-870 nm are derived from direct almucantar measurements and their estimated error varies spectrally from ± 0.01 to ± 0.02 making it a better temporal measurement against satellite AOD measurement, while the AAOD and SSA at 440 nm are inversion products with very minimal error retrieved using the inversion algorithm of AERONET. Radiometric measurements are calibrated using a characterised integrating sphere at GSFC to or greater than an absolute accuracy of 5%, which is found to be fit for satellite radiometric measurement validation.

3.2. MODIS

Moderate resolution Imaging Spectro-radiometer (MODIS) instrument provides near-daily global aerosol product cover-

!t]

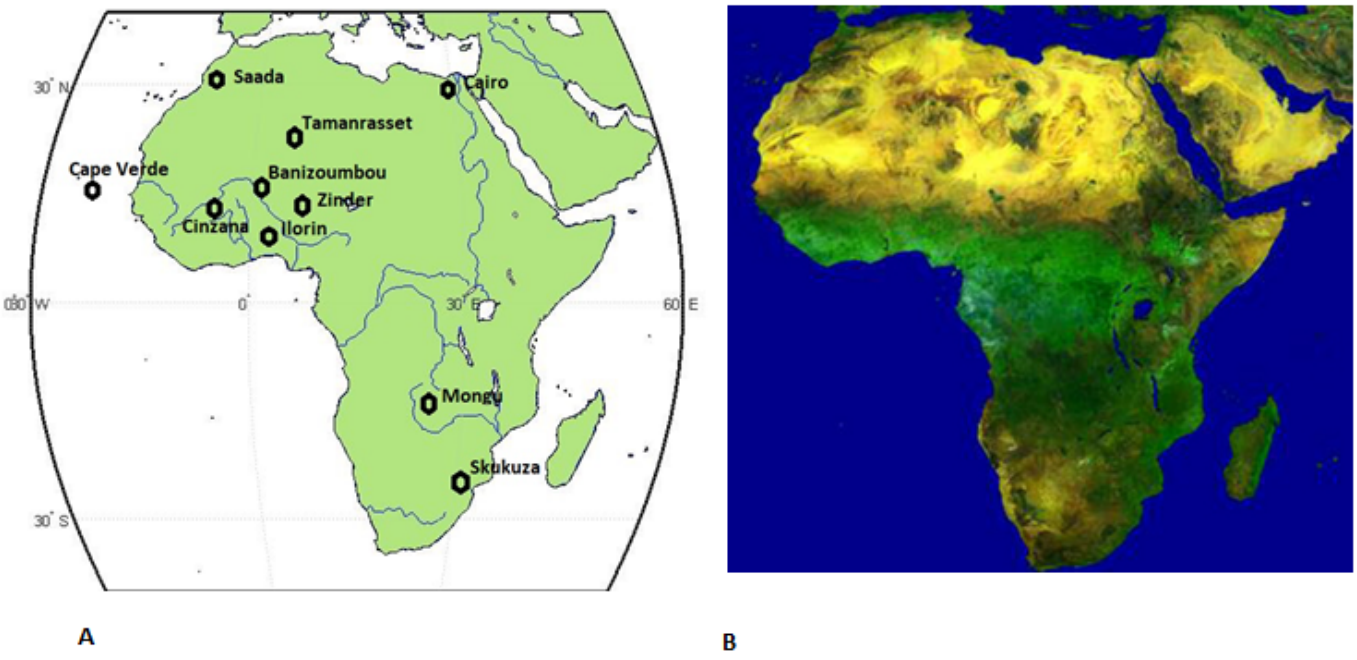

Figure 1. Map of study area (A) Major rivers in blue lines and AERONET sites in black symbol, (B) Vegetation index, surface elevation, and surrounding oceans.

Table 1. Geographical information of AERONET sites in the study.

S/N	AERONET Sites	Country	Latitude Longitude Altitude (m. a.s.l.)	Measurement Duration
1.	Saada	Morocco	31°N 8°W 420	2004-2022
2.	Cairo	Egypt	30°N 31°E 70	2010-2022
3.	Tamanrasset	Algeria	22°N 5°E 1377	2006-2022
4.	Cape Verde	Cape Verde Island	16°N 22°W 60	2000-2022
5.	Banizoumbou	Niger	13°N 2°E 274	2000-2022
6.	Zinder	Niger	13°N 8°E 456	2009-2022
7.	Cinzana	Mali	13°N 5°W 285	2004-2022
8.	Ilorin	Nigeria	8°N 4°E 350	2000-2022
9.	Mongu	Zambia	15°S 23°E 1107	2000-2022
10.	Skukuza	South Africa	24°S 31°E 150	2000-2022

age in the absence of clouds. It has a wide spectral range (0.41μm to 14.5 μm in 36 channels or bands), a broad swath (2330 km), and relatively fine spatial resolution (1km or less depending on band), providing information on atmospheric, terrestrial, and oceanic conditions. Over land, aerosol retrieval is different [39, 40] from over the oceans [41] with higher accuracy on the ocean (±0.03 ± 0.15 (AOD)) than on land (±0.05 ± 0.20 (AOD)). The MODIS AOD retrieval algorithm over land applies three spectral bands at 0.47 μm, 0.66 μm, and 2.1 μm plus those used for cloud masking, and requires that surface-reflected radiation make little contribution to total radiation leaving the top of the atmosphere. The operational MODIS aerosol retrieval algorithms are dark target and deep blue [42] algorithms for vegetated and brighter surfaces, respectively. MODIS aerosol retrieval, which is a downstream L2 product, requires the existence of other L2 products such as geophysical products as well as the L1B product of reflectance for retrieval. The operational MODIS retrieval data are produced and archived by the MODIS Adaptive Processing System (MODAPS; http://modaps.nascom.nasa.gov/services/) and are available online (http://ladsweb.gsfc.nasa.gov). MODIS calibration is supported by the MODIS Characterization Support Team (MCST;https://mcst.gsfc.nasa.gov). The quality and accuracy of downstream retrieved products (including aerosol) are dependent on the accuracy of the calibration of the algorithm's input radiances, of which the MCST reports an accuracy of ±2–3% for typical situations [43]. The present study adopted the combined MODIS dark target and the deep blue land and ocean algorithm for AOD and AE at a spatial resolution of 1° × 1° due to the different nature of land cover of the study area for a period of 23 years (1st January 2000–31st December 2022) to understudy variation, spatial distribution, and trend of aerosol proper-

ties most impacted by climate and can serve as climate change indicator over Africa. The data were sourced using the NASA Giovanni platform: https://giovanni.gsfc.nasa.gov/giovanni/.

3.3. OMI

Ozone Monitoring Instrument (OMI) is a hyper-spectral passive satellite sensor launched on July 15, 2004, into a sun-synchronous polar orbit sponsored by NASA and its collaborators on board the Aura spacecraft. It is a huge area imaging spectrometer with a viewing angle range of 114° across the track, which offers a broad expanse of 2600 km and a spatial resolution of 3km binned to 13 × 24 km^2 with global coverage within one to two days. It measures direct and backscattered solar radiation in the UV to visible range, which is from 264 to 504 nm in the early afternoon hours of 1300 to 1430. It can also monitor cloud pressure and coverage, which can provide information on tropospheric ozone, NO_2 columns, and the distinction between different types of aerosol. OMI adopted two algorithms for retrieving aerosol properties from top-of-atmosphere radiance measurements: the OMAERO aerosol product (multi-wavelength algorithm) and the OMAERUV aerosol product (near-UV algorithm). The latter produces, in addition to aerosol optical properties, absorption aerosol properties such as AAOD and SSA that give information on atmospheric warming due to thermal energy released during absorption processes. The two algorithms were recently unified in the latest version, OMAEROe v003 Details of the description of OMI can be found elsewhere [44–46]and on OMI website (https://aura.gsfc.nasa.gov). For this study, OMI AAOD and SSA daily data at 442 nm and 0.25° spatial resolution of version OMAEROe v003 were accessed through NASA's Giovanni platform and used over the study period of 19 years (2000 to 2022).

3.4. AIRS

Atmospheric Infrared Sounder (AIRS) is on board Aqua satellite and operates on 2378 channels with a footprint of 15 km at the nadir during daytime measurements, crossing the equator in the early afternoon from the southern to the northern hemisphere. It measures some pollutants, such as carbon monoxide, and atmospheric dynamic parameters like air temperature, surface temperature, and pressure, to mention a few, at different altitudes [47]. AIRS gridded air temperature daily data at altitude 850 hpa close to the surface (1000 hpa), being atmospheric aerosol location, at 1° resolution, version AIRS3STD v7.0 in Kelvin (K) was assessed through NASA's Earth Observing System data platform from 2005 to 2022. The AIRS data is at the public domain (https://airs.jpl.nasa.gov) and been used by weather prediction centres around the world to improve their forecast likewise to assess the skill of climate models.

4. Method

It has been established that aerosol CIs, such as the aerosol parameters considered in this study, can be used to estimate variability and trend in aerosol population in the atmosphere. As such, the spatial distributions of the aerosol parameters were under study over the chosen location and period over the long term (2000–2022). This was done using combined MODIS and OMI data at different wavelength bands around 400 nm for AE, AAOD, and SSA, while AOD at 550 nm, all in the visible band. All satellite data were accessed through the Giovanni platform, EarthData version 4.38, at different spatial resolutions (https://giovanni.gsfc.nasa.gov). The details of the data are shown in Table 2. The decadal analyses of the parameters were done using the AERONET dataset over the ten sites selected within the study region to be able to accommodate local aerosol production and the decadal percentage difference is calculated using equation (5).

$$\%\ Diff = \frac{|A_1 - A_2|}{Average} \times 100, \tag{5}$$

where A is the decadal average of the optical properties considered and 1,2 stand for the first and second decades.

The trend is a significant change over time exhibited by a random variable such as aerosol properties, detectable by statistical parametric and non-parametric procedures that can be used interchangeably with identical results in most cases [48, 49]. The AERONET aerosol optical and absorption time series for ten sites in Africa with more than ten years of data are aggregated into monthly time series to observe long-term potential changes and quantify whether trends is significant or insignificant in one sub-region compared to the others. A parametric trend test was adopted in this study using linear regression of the random variable Y (aerosol properties) on time X (month of the year). The regression coefficient β (or the Pearson correlation coefficient) is the interpolated regression line slope coefficient computed from the data, representing the trend estimate of the variable in the considered period. The statistic follows the t-distribution with n-2 degree of freedom, as shown in equation (6).

$$t = \frac{\beta}{\frac{\sum (Y_i - \hat{Y}_i)^2}{(n-2)\sum (X_i - \overline{X})^2}}, \tag{6}$$

where n is the sample size. The null hypothesis H_0: β = 0 (no trend) is tested against the hypothesis H_0: β ≠ 0 (presence of trend) at a chosen level of significance α.The hypothesis that there is no trend is rejected when the t value computed by equation (6) is greater in absolute value than the critical value $t_{\alpha/2}$.

A linear trend model is derived from the regression analysis, using equation (7),

$$Y_i = \beta X_i + c + \varepsilon, \tag{7}$$

where Y_i is the aerosol variable for which the trend is been estimated, β is the trend estimate of the variable, X_i is the independent variable time in months, c is the intercept on the vertical axis and ε is the noise in the time series data.

The significance of the estimated trend is tested using the coefficient of the determinant (R-value) of the curve and the direction of the trend is revealed by the sign preceding the slope. The aerosol variables understudy were compared with a known

Table 2. Sources and attributes of data used in the study.

Parameter	Spatial Resolution	Frequency	Time Period	Source
$AOD_{550\ nm}$	1°×1°	Monthly	2000-2022	MODIS TERRA
$AE_{412-470\ nm}$	1°×1°	Monthly	2000-2022	MODIS TERRA
$AAOD_{442\ nm}$	0.25°×0.25°	Daily	2005-2022	OMI
$SSA_{442\ nm}$	0.25°×0.25°	Daily	2005-2022	OMI
$AOD_{440\ nm}$	Point data	Monthly		AERONET
$AE_{440-870\ nm}$	Point data	Monthly		AERONET
$AAOD_{440\ nm}$	Point data	Monthly		AERONET
$SSA_{440\ nm}$	Point data	Monthly		AERONET
Air Temperature	1°×1°	Monthly	2005 & 2022	AIRS

and popular climate change indicator, air temperature, in the study area at 850 hpa altitude using Pearson correlation in the environment of Godard Space Flight Centre EarthData Application. This was done in other to infer the link and serve as foundation for establishing aerosol climate change indication in the African region

5. Results

5.1. Aerosol properties' distribution and variation

Figure 2 shows some selected year distribution and long term variation of the AOD and AE from MODIS at 1° res., AAOD and SSA from OMI at 0.25° resolution over the African Region within the study period. A high AOD of greater than 0.5 is found and clusters around the west and central Africa bordering the Atlantic Ocean, with patches of very high AOD at the west-central Africa coaster cities and sub-Saharan areas, with a maximum value (< 0.8) at Bodele depression and some major industrial cities. This is associated with both anthropogenic/economic activities of the population and the natural desert dust of the Sahara which is the largest dust source in the world. The low AOD values of ≤ 0.2 are found in the south, Madagascar, and scattered around the far north at the coast of the Mediterranean and East Africa. It is observed that most aerosols are detected close to their source region. Cities like Lagos, Accra, Kano, Abijdan, and other economic cities with dense populations and industries are characterised by rich emission loads. Some remote areas with low activities are situated in aerosol transport routes hence they receive high aerosol loads such as sub-Sahel areas. Mountainous areas suffer aerosol accumulation due to the orographic effect and blockage of long-range transport resulting in low AOD at high altitudes due to high deposition. Aerosol load in large river areas including the basins, lakes, and dams in the study area as shown in Figure 1A depends on the sources such as population, surrounding enclaves and basin effect. AOD averaged over the year 2005, 2010, and 2022 reveal a decreasing trend in aerosol load in almost all the areas of the continent across the years. This is in agreement with other studies in the region and elsewhere for aerosols during the study period and may be attributable to the modernization of technology in the industrial sector, control measures put in place and changes in atmospheric conditions that support the frequent suspension and deposition of the dust particle such as wind system, rainfall, ground wetness, and temperature (air and soil) [50]. The decadal percentage difference of the AOD shows the variation is more of local than a regional event with Ilorin having the highest percent (23.67%) followed by Mongu (13.28%), and Tamanrasset (11.51%) and the least percent at Saada (0.14%) a station in Morocco (Table 4).

AE gives information about the size distribution of the aerosol particles, with the small AE values for coarse mode particles and large values for fine-mode aerosol particles. MODIS observation in Figure 2B shows AE ranges from 0 to 1 over the African region, with small values (≤ 0.35) dominating the north, indicating coarse mode dominance, and larger values (≥ 0.70) dominating the south, indicating fine mode dominance (Table 3). This reveals an anti-relationship with the AOD, indicating the high AOD values observed in the north mainly from the contribution of dust-like particles due to poor vegetation cover. Over the study area, a clear boundary exists between larger AE values in the south and smaller values in the north at the sub-Sahel location, extending from west to east, with some isolated occurrences of larger AE values in the north mainland, surrounding Island and its coaster areas. The coaster areas of Angola and Namibia in the south experienced moderate AE values, which may be from the nearby desert (Kalihari) and what has been transported from central Africa and across the ocean. Reduction in the sizes of the coarse particles in the north is observed in the year 2010 leading to moderate values of AE in the sub-regions with the intrusion of finer mode aerosol from anthropogenic sources. In the year 2022, an improvement in the size of the particles was observed with maxima values to what is experienced in the year 2005 transported south ward. The variation in AE experienced mostly in the north may be associated with mixed emission sources and high deposition rates of largest-size particles through wet or dry deposition [51]. This is justified by the close range of the decadal percentage differences of the selected AERONET sites in the north (3-6%)

except for Cape Verde (0.67%) and Ilorin (18.26%) which may be due to deposition over the ocean and fine mode aerosol received from the south respectively. however, less spatial variation is observed in the south over time due to homogeneity of the nature of the emitted aerosol (smoke).

AAOD is the load of absorbing aerosol in the atmosphere contributing to atmospheric warming through the release of thermal energy during solar energy absorption and its value in the study area ranges from 0 to 0.2 as shown in Figure 2C by OMI. The maximum AAOD was experienced around the Gulf of Guinea and the coast of central Africa extending eastward over Congo D. R which may be ascribed to the percentage of carbon content of the emitted aerosol from the combustion processes, biomass/forest burning, and oil exploration exercise. Other parts of the study area experienced little or no load of absorbing aerosol. This is in agreement with the previous study in the region [6, 52]. The temporal variation between the year 2005 and 2010 shows a reduction in the aerosol maxima areas at the gulf of guinea and partly in the Gabon coast mainly due to measures taken on gas flaring. The maxima shifted to central Africa towards the east extending southward (Mozambique) in the year 2022 with some pocket of maxima values all over the region as a result of economic recovery processes from the shutdown due to the emergence of the COVID-19 pandemic globally [53]. There is a high gap of percentage difference of AAODs within the study area over time as shown in Table 4 which may be due to individual site economic activities or proximity to the industrial hub contributing majorly to the load.

SSA as an attribute of aerosol describing the interaction of particles with shortwave solar radiation in the atmosphere, is as shown in Figure 2D over the study area and it ranges between 0.87 and 0.98. The lesser values indicate high absorption and low scattering while greater values indicate high scattering and low absorption of solar radiation [52]. Absorbing particles (< 0.9) are found around the coast of central Africa extending into the central mainland in the year 2010 with the majority of other areas having scattering particles (> 0.92) with a maximum over the east, Sub-Sahel belt and coast of Mediterranean sea. Over time in 2022 the absorbing particles are found scattered over the other part of the south and some isolated locations in the north with a decrement in the spread of scattering particles compared to the situation in 2010. These may be associated with an increase in human population in the region and activities resulting from it such as deforestation, agricultural/biomass burning and carbonaceous emissions to mention a few. The decadal percentage differences of the SSA for sites within the study area are less varied (0.01-0.91) except Saada (2.02), Cape Verde (1.57), and Cinzana (1.51) (Table 4) revealing their fluctuating behaviour from scattering to absorption and vice versa based on their composition.

5.2. Trends in Aerosol Optical Properties (AOP)

5.2.1. Trend in AOD

The temporal linear regression trends in columnar AOD, AAOD, AE, and SSA and their statistical significance over the chosen ten AERONET sites in the study region within the study period are as shown in the representative figure of Figure 3 and detailed description in Table 5. It is estimated in terms of increasing/decreasing trending values indicated by positive/negative signs respectively. AOD trends in all ten sites representing different climates vary from positive to negative trends with spatial patterns in the northern area than the southern area. Negative trends were observed in the farthest north to the middle of Sahara sites with the temperate and arid climate system respectively and partly significant in the Cairo area. This may be attributed to dry deposition as a result of intense heating bringing about dry convection around the area of inter-tropical discontinuity (ITD) when it is at the upmost position and gravitational settling of the coarse mode aerosol not far from the sources in addition to the deposition over the sea [54–56]. The Sahel area of the study region with four sites of arid, semi-arid, and tropical climates experienced less significant positive trends of AOD indicating high aerosol production with a major contribution from other sources (smoke) aside from dust. It may also be attributed to the lack of rainout of the particles in the atmosphere due to changes in the rainfall trend of the area as reported by previous studies and reports of the united nation organisation on climate change [57, 58].

The Sub-Sahel area in the tropics where Ilorin site lies experienced a negative trend in AOD over time. Wet deposition is the main attributable factor to the decreasing trend of the AOD in the tropical climate. Furthermore, the reduction in anthropogenic emissions from industries, construction sites, vehicles, and domestic cooking due to modern technology and fuel efficiency in recent times has played role in decreasing trend of AOD in addition to the reduction of transported dust load in the cool dry period (harmattan- Dec-Jan-Feb) through the north-easterly trade wind that occupies the area [59]. In the south, the two other sites fall into the temperate climate system, with less rainfall compared to the tropical climate. Mongu is in the central south, while Skukuza is situated in the north of the South African Republic. The positive trend of AOD is observed in the central part of the south, which is very insignificant. This may be due to seasonal anthropogenic emission from biomass/agricultural burning of the locals and aged transported smoke from the biggest smoke hotspot in Africa (Congo D. R.) year-round and across the Indian Ocean [6]. A negative AOD trend was experienced in the southernmost site in a controlled human activity area. The control of anthropogenic activities in the area over the long-term serves as a major factor influencing the decrease in the aerosol load which in turn leads to AOD downward trend.

5.2.2. Trend in AE

Angstrom Exponent describes the particle size distribution in a negative relationship, and aerosol composition is the major factor determining the AE value. AE trends in the region during the period under study are negative except for Zinder and Ilorin in the semi-arid and tropical climates, respectively, which are positive. The decreasing trend in the majority of the sites indicates a reduction in the population of fine mode particles in the air, which is significant in some parts of the region, such as

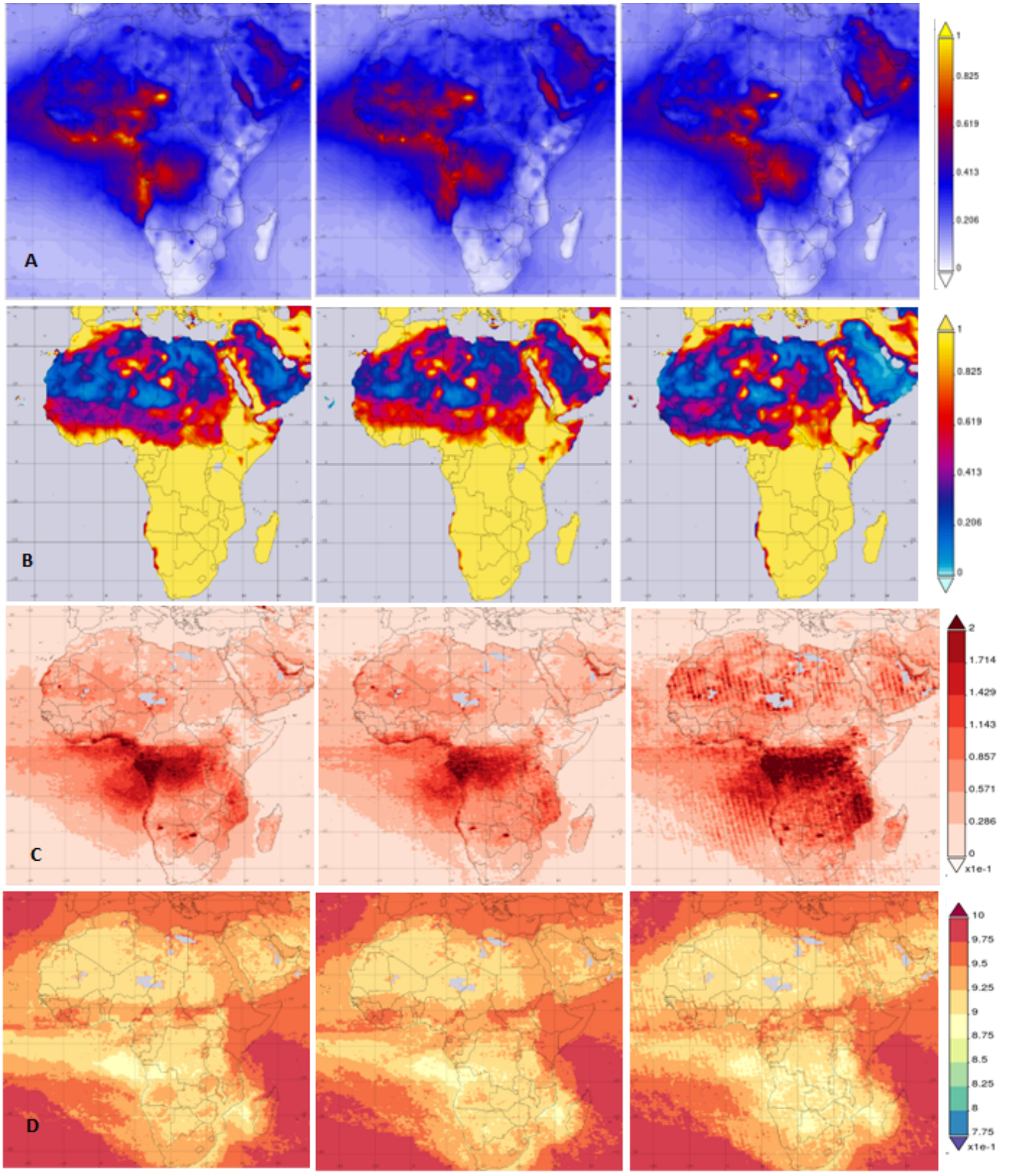

Figure 2. Variability in distribution of (A) AOD, (B) AE, (C) AAOD, and (D) SSA for the year 2005 (left), 2010 (midle), and 2022 (right).

the north-eastern area (Cairo). This may be due to a decrease in anthropogenic emissions such as sulphate, smoke, and VOCs, to mention a few, which are made up of fine mode aerosols, as a result of control measures put in place to check their emissions

Table 3. Decadal average of AERONET aerosol optical properties.

S/N	Location	First Decade				Second Decade			
		AOD 440 nm	AE 440-870 nm	AAOD 440 nm	SSA 440 nm	AOD 440 nm	AE 440-870 nm	AAOD 440 nm	SSA 440 nm
1.	Cairo	.44±.01	.97±.07	.07±.01	.87±.01				
2.	Saada	.21±.05	.78±.14	.04±.01	.91±.01	.21±.02	.73±.11	.05±.01	.89±.02
3.	Tamanrasset	.25±.08	.37±.15	.06±.01	.89±.01	.22±.07	.38±.10	.06±.01	.89±.01
4.	Cape Verde	.35±.02	.26±.04	.06±.01	.91±.01	.34±.03	.26±.04	.04±.01	.92±.01
5.	Banizoubou	.51±.06	.35±.02	.07±.01	.89±.02	.49±.05	.34±.08	.06±.00	.90±.01
6.	Cinzana	.43±.04	.34±.04	.07±.01	.89±.01	.45±.04	.32±.03	.07±.03	.88±.04
7.	Zinder	.50±.04	.33±.06	.06±.01	.90±.01	.55±.07	.35±.01	.06±.00	.89±.01
8.	Ilorin	.78±.33	.67±.09	.13±.01	.87±.01	.61±.07	.81±.17	.12±.03	.87±.01
9.	Mongu	.27±.01	1.55±.13	.08±.01	.87±.01	.31±.09	1.43±.21	.08±.01	.87±.02
10.	Skukuza	.25±.03	1.29±.15	.07±.02	.89±.01	.23±.02	1.25±.09	.07±.00	.88±.00

Table 4. Decadal percentage difference of AERONET aerosol optical properties.

Location	Decadal percentage difference (%)			
	AOD 440 nm	AE 440-870nm	AAOD 440 nm	SSA 440 nm
Cairo				
Saada	0.14	5.76	21.03	2.02
Tamanrasset	11.51	3.86	4.20	0.01
Cape Verde	4.99	0.67	25.27	1.57
Banizoubou	3.44	4.95	8.73	0.60
Cinzana	1.34	6.99	10.09	1.51
Zinder	8.88	5.56	2.43	0.91
Ilorin	23.67	18.26	9.04	0.87
Mongu	13.28	8.00	3.41	0.29
Skukuza	8.33	2.68	2.09	0.81

for the realisation of SDG goals, and this is in agreement with the study of Eck *et al*. [46]. The areas that experienced positive trends experienced the opposite that is fine mode aerosol population increases due to high anthropogenic emissions mostly from biomass burning for agricultural purposes.

5.2.3. Trend in AAOD

The trend in AAOD over the African region is varied, showing positive and negative values based on absorbing components of the aerosol, such as the carbon content or type of minerals in the dust aerosol. The Mediterranean border (Cairo and Saada sites) experienced a significant positive trend with average AAOD values. The positive trend observed may be attributable to the soot from the economic activities of the area and that of Europe being transported down, aided by the prevailing meteorological conditions such as high humidity and land and sea breeze circulation. The central Sahara (Tamanrasset) is dominated by a negative trend of AAOD, signifying a reduction in the absorbing mineral content of dust, the sole aerosol source of the area, such as quartz, hematite, and clay, which exhibit strong absorption in the blue wavelength region (440 nm) [6, 60]. The Sahel area exhibits varying trends, positive to the east (Zinder) and negative to the west (Cape Verde). This may be as a result of varying mixtures of the aerosol in the area, specifically dust and smoke (brown carbon from biomass burning), depending on the highest percentage aerosol type, with the net effect of stronger absorption, as reported by Russell *et al* [61]. AAOD in the sub-Sahel (Ilorin) exhibits a negative trend due to a reduction in the smoke emitted from bush burning over time and the seasonal rainfall cycle, while the central south (Mongu) experienced a positive trend basically as a result of improved biomass burning due to the agricultural activities of the population. The Skukuza site in South Africa experiences a negative trend in AAOD because the area is under control against bush and forest fires because it is a national park and the impact of the measure is shown in the trend despite being in a smoke-dominated region and close to the administrative capital Pretoria.

5.2.4. Trend in SSA

The single scattering albedo of aerosol particles is a function of both the composition and size of the aerosols; mixed aerosol types with different sizes and compositions can produce complex single scattering albedos, as reported by Giles *et al*. [4]. In the trend of SSA over the study area, there is more of a pattern in the north than the south, with varying signs. The Mediterranean coast area exhibits negative trends over time, signifying improvement in the load of fine mode aerosol, reduc-

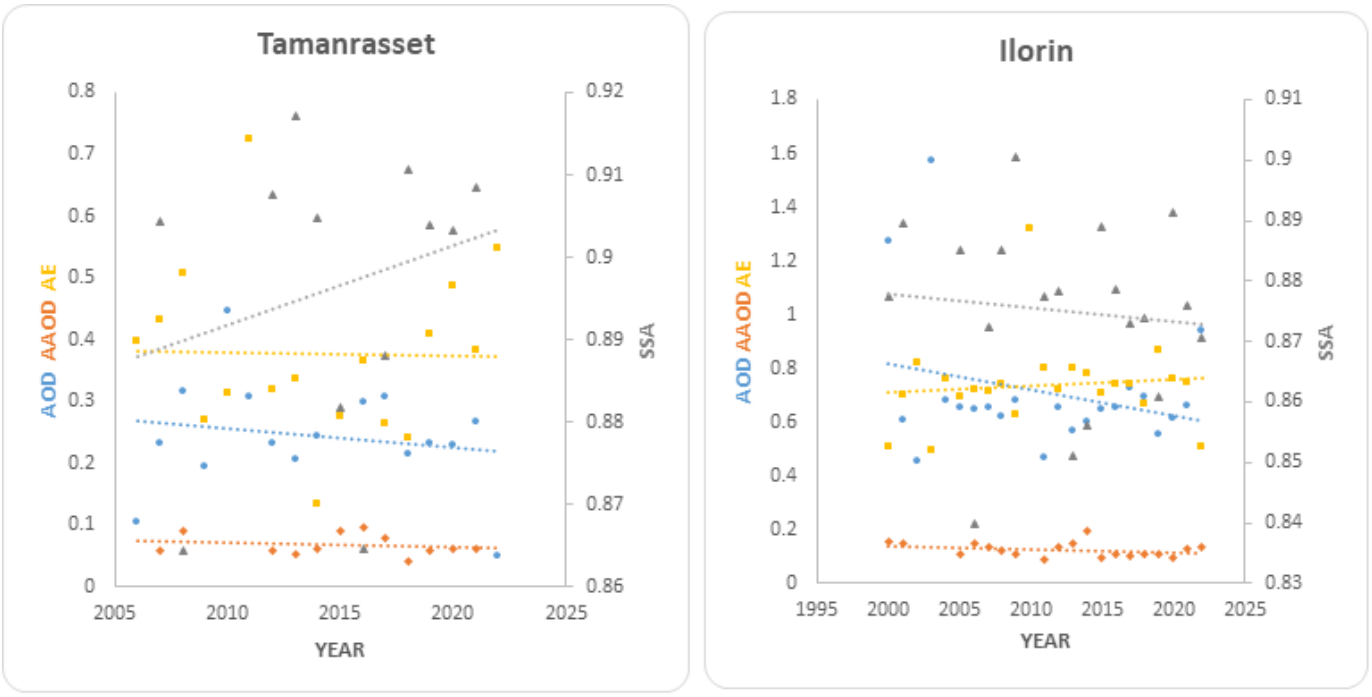

Figure 3. Sample of temporal trends of monthly mean of AOD, AE, AAOD and SSA within the study period (2000-2022).

ing the scattering efficiency of dominant aerosol. This could be attributed to the urbanisation in the area and the incursion of sulphate smoke from industrialised nations in Europe as well as from conflict zones nearby in the Middle East. Down in the middle of the Sahara, the trend switched to positive, indicating high emission of coarse mode aerosol from the desert, which may be a result of changes in the meteorological conditions of the environment [19]. There is a variation of trends within the Sahel belt, with positive trends in Cape Verde and Banizoubou and negative trends in Cinzana and Zinder. This complex trend behaviour is highly likely due to the nature of the aerosol mixture in the area and the external mixing of different aerosol particle sizes attributable to different aerosol sources in the area [6]. Furthermore, the sub-Sahel and farthest south experience negative SSA trends, while the central south has no such phenomenon. The negative trends indicate less coarse mode particles (dust) intruding into the sites from neighbouring Bodele depression and Kalihari deserts respectively while no trend situation in the central south may be associated with persistent burning and deforestation in the area over the years.

5.3. Air temperature-climate change indicator link with aerosol properties

Of all the climate change indicators according to previous studies, temperature exerts the highest influence on AOD through atmospheric photochemical effects like the gas-to-particle conversion process, leading to more particles in the air [17, 55]. Also, the majority of the climate crisis has been fuelled by rising temperatures such as deadly extreme rainfall or storms, excessively prolonged drought, frequent forest fires and glacier melting leading to sea level rise, and the temperature has been predicted to continue to rise by the United Nations Climate Agency (COP). All these lead to investigating the air temperature link with aerosol properties studied over the study area in the long term as prescribed by literatures [62, 63], so as to establish aerosol-CI in the region. If the correlation value (r) is 1, it is perfectly positive. Correlation is strongly positive if $1 > r \geq 0.6$, moderately positive if $0.6 > r > 0.2$, and $r \leq 0.2$ is a positive weak correlation with all signalling positive relationship. If the correlation r is negative it simply signifies a negative relationship in the like manner.

5.3.1. Air Temperature (T) with AOD

Figure 4 shows the spatial correlation between temperature-CI versus AOD, AE, AAOD and SSA for the years 2005 and 2022. There exist isolated scattered perfect positive correlation (> 0.95) of AOD and T with strong correlation serving as background from north-west to the north-east areas including the Cape Verde Island and the central southern Africa, improving over time (Figure 4A & 4B). At the Sahel, there are pockets of negative correlation that are surrounded with weak positive correlations and over time swung to positive ones. This may be due to micro climatic effect of high aerosol emission arising from dust liberation from desert influenced by sub regional long range transportation. Weak and moderate positive correlations dominated the other part of the continent with negative correlation spreading across the central and east Africa reducing in magnitude and spread in 2022. The negative correlation observed is as result of very low aerosol load in the central and eastern belt extending south to the coast of Indian Ocean. The Island of Madagascar experienced decreasing positive correlation with negative one taking over in recent time, it may be as-

Table 5. Trends of Aerosol properties observed in the ten AEROET sites of study area.

S/N	Sites	Parameters	Trend Type	B (ρ>0.05)	R	Remark
1	Cairo	AE	Negative	0.0153	0.577	Significant
		SSA	Negative	0.0004	0.792	Significant
		AOD	Negative	0.0033	0.454	Significant
		AAOD	Positive	0.0019	0.527	Significant
2	Saada	AE	Negative	0.0048	0.186	Insignificant
		SSA	Negative	0.0018	0.439	Significant
		AOD	Negative	0.0002	0.001	Insignificant
		AAOD	Positive	0.0011	0.407	Significant
3	Tamanrasset	AE	Negative	0.0005	0.02	Insignificant
		SSA	Positive	0.001	0.240	Insignificant
		AOD	Negative	0.0031	0.177	Insignificant
		AAOD	Negative	0.0007	0.192	Insignificant
4	Cape Verde	AE	Negative	0.0008	0.044	Insignificant
		SSA	Positive	0.0006	0.234	Insignificant
		AOD	Positive	0.0006	0.102	Insignificant
		AAOD	Negative	0.0002	0.081	Insignificant
5	Banizoubou	AE	Negative	0.0015	0.155	Insignificant
		SSA	Positive	0.005	0.174	Insignificant
		AOD	Positive	0.0021	0.169	Insignificant
		AAOD	Negative	0.0005	0.24	Insignificant
6	Cinzana	AE	Negative	0.0027	0.312	Insignificant
		SSA	Negative	0.0012	0.194	Insignificant
		AOD	Positive	0.0002	0.024	Insignificant
		AAOD	Positive	0.001	0.198	Insignificant
7	Zinder	AE	Positive	0.0041	0.294	Insignificant
		SSA	Negative	0.0018	0.557	Significant
		AOD	Positive	0.006	0.384	Insignificant
		AAOD	Positive	0.0008	0.338	Insignificant
8	Ilorin	AE	Positive	0.0024	0.103	Insignificant
		SSA	Negative	0.0002	0.103	Insignificant
		AOD	Negative	0.0095	0.261	Insignificant
		AAOD	Negative	0.0013	0.323	Insignificant
9	Mongu	AE	Negative	0.0072	0.24	Insignificant
		SSA	Neutral	0.0000	0.002	No trend
		AOD	Positive	0.0008	0.07	Insignificant
		AAOD	Positive	0.0002	0.08	Insignificant
10	Skukuza	AE	Negative	0.0057	0.266	Insignificant
		SSA	Negative	0.0005	0.230	Insignificant
		AOD	Negative	0.0018	0.337	Insignificant
		AAOD	Negative	0.0003	0.095	Insignificant

sociated with constant low AOD and moderate temperature in the area with majority of the Island surface covered with vegetation limiting the dust emission year round (Figure 1B).

5.3.2. *T with AE*

In the case of T and AE, scattered weak positive correlations were observed at the southern and eastern areas including Madagascar which may be associated with fresh and aging smoke plume of high AE values emitted from forest fire and agricultural activities in the areas. There exist improvement in the relations of the variables over the economic and coaster cities of West Africa over time revealing increase in industrial emission. The other part of the study areas were dominated with strong and weak negative correlation (Figure 4C & 4D) signifying dominance of particles of small AE values of either dust or mixed aerosol particles.

5.3.3. *T with AAOD*

A scattered strong positive correlation (0.8) was observed around the island of Izana in the North Atlantic Ocean (Morocco area) in the year 2005 (Figure 4E), with a moderate positive correlation (0.4) at the background spreading eastward in

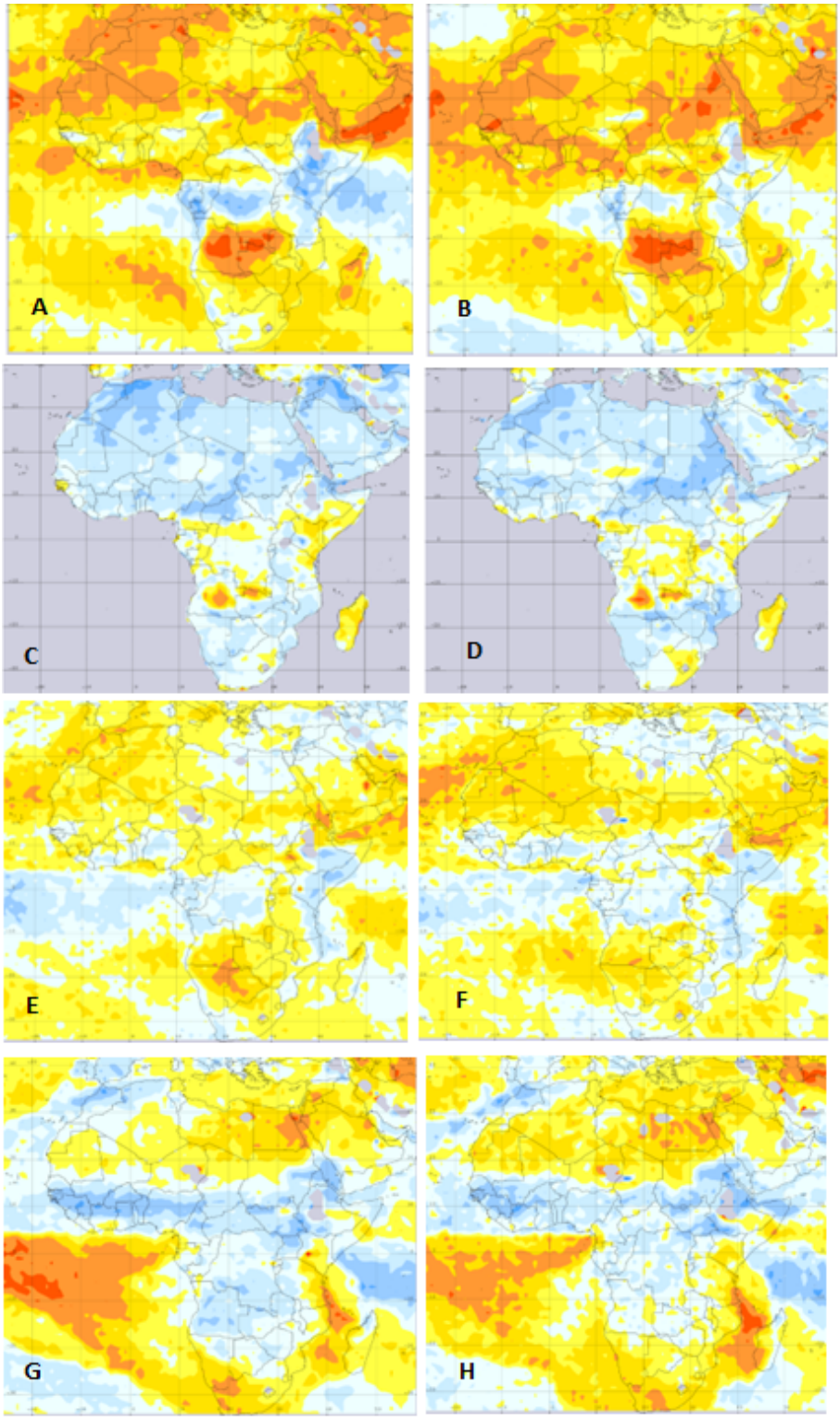

Figure 4. Spatial correlation (A & B) AOD vs T, (C & D) AE vs T, (E & F) AAOD vs T, and (G & H) SSA vs T for the year 2005 (left) and 2022 (right).

the mainland and improving over time (2022-Figure 4F). The Egypt area in the east on the Mediterranean coast experienced a negative correlation, which reduced in spatial coverage by the year 2022, with a weak positive correlation taking over. This is a result of the disparity between their composition and radiative forcing, i.e., high absorption particles to the west and less absorbing ones to the east have gradually been replaced and are contributing to the rise in temperature through the thermal

energy released during the emission of long wave solar radiation [59]. In the Sub-Sahara, from the South Atlantic Ocean in the west to east Africa in 2005, a negative correlation between AAOD and air temperature dominated the sub region, with scattered weak positive correlations. The negative relationship spread, eliminating the weak positive correlation in the sub-region in 2022 and having an anti-relationship to the far northern situation. This can be associated with the negative trends of AAOD in the area as a result of reduced anthropogenic emissions of smoke dominating the area. In the south, there are strong and moderate positive correlations at the centre opposite the Namibia desert, as shown in Figure 4E. It reduced to only moderate once and shifted partly to the Atlantic, surrounded by a weak correlation extended to Madagascar over time (Figure 4F). This is opposite to the correlation behaviour in the far north with improving positive correlation strength and may be due to the presence of more scattering aerosols likely from the nearby desert (Kalihari) mixing the absorbing aerosol of the area causing less impact on atmospheric warming.

5.3.4. T with SSA

Strong negative relation was observed at the Sub-Sahel belt which reduces to a moderate negative ones in the year 2022. South Atlantic Ocean experienced perfect positive correlation with a strong one in the background and surrounded by a weak correlation stretching to the Gulf of Guinea (Figure 4G & 4H). In the mainland weak negative correlation spread to the south with the tip of Cape and Madagascar having a strong positive correlation improving over time. Sizes of the particles determine the types of the scattering which can be forward scattering contributing to atmospheric radiation as much as warming up the air which in turn increases the air temperature in the perfect and strong positive correlation areas. The other sizes that were involved in backward scattering sent some radiation back to space thereby reducing the amount of atmospheric radiation that could warm up the air resulting in an anti-relationship with the air temperature as shown in the south of the study area.

6. Conclusion

The study presents the analysis of spatial variability and temporal trends in aerosol properties over Africa as detected by MODIS, OMI, and AERONET during the year 2000 to 2022 and with established temperature-climate change indicator from AIRS at altitude 850 hpa to improve the understanding of aerosol-based climate change indicator in the region. The spatial distribution of AOD, AE, AAOD, and SSA in the study region were characterised as high, moderate and low which varied with time and local emissions playing key roles. The High aerosol load observed in west-central Africa and their coaster areas were reduced over time for AOD and improving for AAOD mostly in the north of southern Africa. The size and scattering attributes of the aerosol varied based on the aerosol type such as dust, smoke, sea salt and the source region which in turns determine its impact on air temperature. Trends in AOD are on a significant decrease in the arid area of the north and an increase in the arid Sahel and central Africa while the southern area is on a decreasing trends. The study area is dominated by negative trends in AAOD except for southern central Africa having a significant positive trend and the east of Sahel attributed to intense bush burning and reduction in soil moisture leading to more suspension of soil particles. AE trends during the study period are on the decrease except for the sub-Sahel area, indicating a significant load of fine particles from anthropogenic activities. The SSA trended positively from the middle of the Sahara through Banizoubou to the island of Cape Verde in the Atlantic Ocean, indicating the presence of pure dust in the area suspected to be from the dust hotspot of central Sahara. Other parts of the study area experienced a negative trend except for Mongu in the central south, which had a neutral trend. These reveal the consistent increase in anthropogenic emissions due to economic or agricultural activities. There is a strong relationship between air temperature, a popular climate change indicator and all the variables considered with the exception of AE having dominance negative correlation, which either improved or decreased over different areas based on the level of aerosol load and composition. Variation and trend studies of aerosol properties like thsse in this research could greatly contribute to aerosol load detection and quantification of its effects on climate through radiative forcing and human health through air quality that the monitoring is limited on the African continent.

Data availability

The dataset used in this study was adopted from NASA Godard Space Flight Centre AERONET, MODIS, and OMI and their respective links is as follows; https://aeronet.gsfc.nasa.gov, http://ladsweb.gsfc.nasa.gov, and https://aura.gsfc.nasa.gov.

Acknowledgments

We would like to thank the Moderate resolution Imaging Spectro-radiometer (MODIS), Ozone Monitoring Instrument (OMI) and Atmospheric Infrared Sounder (AIRS) characterization support teams for their extensive efforts in maintaining the high radiometric quality of satellite based data. AERONET team, supported by the NASA EOS project office and the Radiation Sciences Programme, is gratefully acknowledged for calibration and processing of data, as well as the principal investigators of the selected sites with their respective site managers for continuous maintenance of the equipment on site. The support of our various institutions is acknowledged.

References

[1] IPCC, "Summary for policymakers", in *Climate change 2021: The physical science basis, contribution of working group i to the sixth assessment report of the intergovernmental panel on climate change*, V. Masson-Delmotte, P. Zhai, A. Pirani, S.L. Connors, C. Péan, S. Berger, N. Caud, Y. Chen, L. Goldfarb, M.I. Gomis, M. Huang, K. Leitzell, E. Lonnoy, J.B.R. Matthews, T.K. Maycock, T. Waterfield,

O. Yelekçi, R. Yu & B. Zhou (Ed.), Sixth Repo, Swizerland, 2021, pp. 3–216. https://www.ipcc.ch/report/ar6/wg1/downloads/report/IPCC_AR6_WGI_SummaryVolume.pdf.

[2] V. Ramanathan, "Indian Ocean Experiment: An integrated analysis of the climate forcing and effects of the great Indo-Asian Haze", Journal of Geophysical Research **106** (2001) 28371. https://doi.org/10.1029/2001JD900133.

[3] J. Huang, C. Zhang & J. M. Prospero, "Large-scale effect of aerosols on precipitation in the West African Monsoon region", Q. J. R. Meteorol. Soc. **135** (2009) 581. https://doi.org/doi:10.1002/qj.391.

[4] D. M. Giles, B. N. Holben, T. F. Eck, A. Sinyuk, A. Smirnov, I. Slutsker, R. R. Dickerson, A. M. Thompson & J. S. Schafer, "An analysis of AERONET aerosol absorption properties and classifications representative of aerosol source regions", Journal of Geophysical Research: Atmospheres **117** (2012) 1. https://doi.org/10.1029/2012JD018127.

[5] S. Bibi, K. Alam, F. Chishtie & H. Bibi, "Characterization of absorbing aerosol types using ground and satellites based observations over an urban environment", Atmospheric Environment 150 (2017) 126. https://doi.org/10.1016/J.ATMOSENV.2016.11.052.

[6] S. S. Aladodo, C. O. Akoshile, T. B. Ajibola, M. Sani, O. A. Iborida & A. A. Fakoya, "Seasonal tropospheric aerosol classification using aeronet spectral absorption properties in African locations", Aerosol Science and Engineering **6** (2022) 246. https://doi.org/10.1007/s41810-022-00140-x.

[7] IPCC, "Cimate change 2013: The physical science basis:Working group I contribution to the fifth assessment report of the IPCC", [Online], 2013. https://www.ipcc.ch/report/ar5/wg1/.

[8] J. M. Prospero, W. M. Landing & M. Schulz, "African dust deposition to Florida: Temporal and spatial variability and comparisons to models", Journal of Geophysical Research: Atmospheres **115** (2010) D13304. https://doi.org/10.1029/2009JD012773.

[9] O. Dubovik, B. Holben, T. F. Eck, A. Smirnov, Y. J. Kaufman, M. D. King, D. Tanré & I. Slutsker, "Variability of absorption and optical properties of key aerosol types observed in worldwide locations", Journal of the Atmospheric Science **59** (2002) 590. http://dx.doi.org/10.1175/1520-0469(2002)059%3C0590:VOAAOP%3E2.0.CO;2.

[10] A. Angstrom, "The parameters of atmospheric turbidity", Willey **16** (1964) 64. https://doi.org/10.1111/j.2153-3490.1964.tb00144.x.

[11] A. Matzarakis & B. Amelung, "Physiological equivalent temperature as indicator for impacts of climate change on thermal comfort of humans", in *Seasonal Forecasts, Climatic Change and Human Health*, M.C. Thomson, (Ed.), Springer, Dordrecht, Netherlands, 2008, pp. 161–172. https://doi.org/10.1007/978-1-4020-6877-5_10.

[12] R. C. Sullivan, R. C. Levy, A. M. Silva & S. C. Pryor "Developing and diagnosing climate change indicators of regional aerosol optical properties", Scientific Reports **7** (2017) 1. https://doi.org/10.1038/s41598-017-18402-x.

[13] T. R. Karl, R. W. Knight, D. R. Easterling & R. G. Quayle, "Indices of climate change for the United States", Bull. Am. Meteorol. Soc. **77** (1996) 279. https://doi.org/10.1175/1520-0477(1996)077%3C0279:IOCCFT%3E2.0.CO;2.

[14] J. M. Melillo, T. T. Richmond & G. Yohe, "Climate change impacts in the United States: Third National Climate Assessment", US Global Change Research Program, Washington, D.C, United State, 2014, pp. 234–267. https://doi.org/10.7930/J0Z31WJ2.

[15] B. Marticorena, J. Haywood, H. Coe, P. Formenti, C. Liousse, M. Mallet & J. Pelon, "Tropospheric aerosols over West Africa : highlights from the AMMA international program", Atmospheric Science Letter **12** (2011) 19. https://doi.org/10.1002/asl.322.

[16] J. M. Haywood, J. Pelon, P. Formenti, N. A. Bharmal, M. E. Brooks, G. Capes, P. Chazette, C. Chou, S. A. Christopher, H. Coe, J. Cuesta, Y. Derimian, K. Desboeufs, G. Greed, M. Harrison, B. Heese, E. J. Highwood, B. Johnson, M. Mallet, B. Marticorena, J. Marsham, S. Milton, G. Myhre, S. R. Osborne, D. J. Parker, J. L. Rajot, M. Schulz, A. Slingo, D. Tanré & P. Tulet, "Overview of the dust and biomass-burning experiment and African monsoon multidisciplinary analysis special observing period-0", Journal of Geophysical Research Atmospheres **113** (2008) 1. https://doi.org/10.1029/2008JD010077.

[17] G. Capes, B. Johnson, G. Mcfiggans, P. I. Williams, J. Haywood & H. Coe, "Aging of biomass burning aerosols over West Africa : Aircraft measurements of chemical composition , microphysical properties, and emission ratios", Journal of Geophysical Research **113** (2008) 1. https://doi.org/10.1029/2008JD009845.

[18] K. E. Ukhurebor, S. O. Azi, U. O. Aigbe, R. B. Onyancha & J. O. Emegha, "Analyzing the uncertainties between reanalysis meteorological data and ground measured meteorological data", Measurement **165** (2020) 108110. http://dx.doi.org/10.1016/j.measurement.2020.108110.

[19] G. W. Khamala, J. W. Makokha, R. Boiyo & K. R. Kumar, "Long - term climatology and spatial trends of absorption, scattering , and total aerosol optical depths over East Africa during 2001 – 2019", Environmental Science and Pollution Research **29** (2022) 61283. https://doi.org/10.1007/s11356-022-20022-6.

[20] X. Yu, J. Nichol, K. H. Lee, J. Li & M. S. Wong, "Analysis of long-term aerosol optical properties combining AERONET sunphotometer and satellite-based observations in Hong Kong", Remote Sens. **14** (2022) 5220. https://doi.org/10.3390/rs14205220.

[21] Z. Y. Zhang, M. S. Wong & J. Nichol, "Global trends of aerosol optical thickness using the ensemble empirical mode decomposition method", Int. J. Climatol. **36** (2016) 4358. http://dx.doi.org/10.1002/joc.4637.

[22] S. Ramachandran & M. Rupakheti, "Trends in the types and absorption characteristics of ambient aerosols over the Indo-Gangetic Plain and North China Plain in last two decades", Sci. Total Environ. **831** (2022) 154867. https://doi.org/10.1016/j.scitotenv.2022.154867.

[23] R. K. Boiyo, R. Kumar & T. Zhao, "Spatial variations and trends in AOD climatology over East Africa during 2002–2016: a comparative study using three satellite data sets", Int J Climatol **38** (2018) e1221. https://doi.org/10.1002/joc.5446.

[24] M. Aklesso, R. K. Kumar, L. Bua & R. Boiyo, "Analysis of spatial- temporal heterogeneity in remotely sensed aerosol properties observed during 2005–2015 over three countries along the Gulf of Guinea Coast in Southern West Africa", Atmos Environ **182** (2018) 313. http://dx.doi.org/10.1016/j.atmosenv.2018.03.062.

[25] K. R. Kumar, N. Kang, V. Sivakumar & D. Griffith, "Temporal characteristics of columnar aerosol optical properties and radiative forcing (2011-2015) measured at AERONET's Pretoria_CSIR_DPSS site in South Africa", Atmos Environ **165** (2017) 274. https://doi.org/10.1016/j.atmosenv.2017.06.048.

[26] R. Singh, V. Singh, A. Sagar, G. Sneha, G. Manish, S. Pushpendra & S. Soni, "Temporal and spatial variations of satellite based aerosol optical depths , angstrom exponent , single scattering albedo , and ultraviolet aerosol index over five polluted and less polluted cities of Northern India : Impact of urbanization and clima", Aerosol Science and Engineering **7** (2022) 131. https://doi.org/10.1007/s41810-022-00168-z.

[27] O. A. Falaiye, T. O. Aro & E. B. Babatunde, "Interannual variation of ambient aerosol optical depth at Ilorin a central state of Nigeria", Zuma Journ of Pure and Appl. Sci **5** (2003) 197. https://doi.org/10.1007/s41810-022-00168-z.

[28] G. Snider, C. L. Weagle, K. K. Murdymootoo, A. Ring, Y. Ritchie, E. Stone, A. Walsh, C. Akoshile, N. X. Anh, R. Balasubramanian, J. Brook, F. D. Qonitan, J. Dong, D. Griffith, K. He, B. N. Holben, R. Kahn & N. Lagrosas, "Variation in global chemical composition of PM 2 . 5 : emerging results from SPARTAN", Atmos. Chem. Phys. **16** (2016) 9629. https://doi.org/10.5194/acp-16-9629-2016.

[29] K. D. Perry, T. A. Cahill, R. A. Eldred, D. D. Dutcher & T. E. Gill, "Long-range transport of North African Dust to the eastern United States", Journal of Geophysical Research-Atmospheres **102** (1997) 11225. https://doi.org/10.1023/A:1005277214288.

[30] C. L. Mcconnell, *Aircraft Measurements of Saharan Mineral Dust*, University of Reading, Reading, UK, 2009. https://www.met.reading.ac.uk/~jp902366/research/Claire_McConnell_thesis_090601.pdf.

[31] R. Boiyo, K. R. Kumar, T. Zhao & Y. Bao, "Climatological analysis of aerosol optical properties over East Africa observed from space-borne sensors during 2001 – 2015", Atmospheric Environment **152** (2016) 298. https://doi.org/10.1016/j.atmosenv.2016.12.050.

[32] J. Janowiak, "An Investigation into interannual rainfall variability in Africa", Journal of Climate **1** (1988) 240. https://www.jstor.org/stable/44363714.

[33] B. N. Holben, I. Slutsker, A. Smirnov, A. Sinyuk, J. Schafer, D. Giles, O. Dubovik & U. S. T. De Lille, AERONET ' s Version 2 . 0 quality assurance criteria", the International Society for Optical Engineering **6408** (2006) 1. http://dx.doi.org/10.1117/12.706524.

[34] A. Smirnov, B. N. Holben, T. F. Eck, O. Dubovik & I. Slutsker, "Cloud screening and quality control algorithms for the aeronet database", Re-

mote Sensing of Environment **73** (2000) 337. https://doi.org/10.1016/S0034-4257(00)00109-7.

[35] O. Dubovik, A. Sinyuk, T. Lapyonok, B. N. Holben, M. Mishchenko, P. Yang, T. F. Eck, H. Volten, O. Muñoz, B. Veihelmann, W. J. van der Zande, J. F. Leon, M. Sorokin & I. Slutsker, "Application of spheroid models to account for aerosol particle nonsphericity in remote sensing of desert dust", Journal of Geophysical Research Atmospheres **111** (2006) 1. https://doi.org/10.1029/2005JD006619.

[36] O. Dubovik & D. M. King, "A flexible inversion algorithm for retrieval of aerosol optical properties from Sun and sky radiance measurements", Journal of Geophysical Research Atmospheres **105** (2000) 20673. https://doi.org/10.1029/2000JD900282.

[37] D. M. Giles, A. Sinyuk, M. G. Sorokin, J. S. Schafer, A. Smirnov, I. Slutsker, T. F. Eck, B. N. Holben, J. R. Lewis, J. R. Campbell, E. J. Welton, S. V. Korkin & A. I. Lyapustin, "Advancements in the Aerosol Robotic Network (AERONET) Version 3 database - Automated near-real-time quality control algorithm with improved cloud screening for Sunphotometer aerosol optical depth (AOD) measurements", Atmos. Meas. Tech. **12** (2019) 169. https://doi.org/10.5194/amt-12-169-2019.

[38] A. Sinyuk, O. Dubovik, B. Holben, T. F. Eck, F. Breon, J. Martonchik, R. Kahn, D. J. Diner, E. F. Vermote, J. Roger, T. Lapyonok & I. Slutsker, "Simultaneous retrieval of aerosol and surface properties from a combination of AERONET and satellite data", Remote Sensing of Environment **107** (2007) 90. https://doi.org/10.1016/j.rse.2006.07.022.

[39] A. M. Sayer, N. C. Hsu, C. Bettenhausen & M. Jeong, "Validation and uncertainty estimates for MODIS Collection 6 Deep Blue, aerosol data", Journal of Geophysical Research: Atmospheres **118** (2013) 7864. https://doi.org/10.1002/jgrd.50600.

[40] Y. J. Kaufman, D. Tanré, H. R. Gordon, T. Nakajima, J. Lenoble, R. Frouin, H. Grassl, B. M. Herman, M. D. King & P. M. Teillet, "Passive remote sensing of tropospheric aerosol and atmospheric correction for the aerosol effect", Journal of Geophysical Research: Atmospheres **102** (1997) 16815. https://doi.org/10.1029/97JD01496.

[41] D. Tanre, Y. J. Kaufman, M. Herman & S. Mattoo, "Remote sensing of aerosol properties over oceans using the MODIS/EOS spectral radiances", J. Geophys. Res **102** (1997) 16971. http://dx.doi.org/10.1029/96JD03437.

[42] N. C. Hsu, M. J. Jeong, C. Bettenhausen, A. M. Sayer, R. Hansell, C. S. Seftor, J. Huang & S. C. Tsay, "Enhanced Deep Blue aerosol retrieval algorithm: The second generation", Journal of Geophysical Research Atmospheres **118** (2013) 9296. https://doi.org/10.1002/jgrd.50712.

[43] R. C. Levy, S. Mattoo, L. A. Munchak, L. A. Remer, A. M. Sayer, F. Patadia & N. C. Hsu, "The Collection 6 MODIS aerosol products over land and ocean", Atmos. Meas. Tech **6** (2013) 2989. https://doi.org/10.5194/amt-6-2989-2013.

[44] O. Torres, P. K. Bhartia, H. Jethva & C. Ahn, "Impact of the ozone monitoring instrument row anomaly on the long-term record of aerosol products", Atmos Meas Tech **11** (2018) 2701. https://doi.org/10.5194/amt-11-2701-2018.

[45] A. J. Adesina, K. R. Kumar, V. Sivakumar & S. J. Piketh, "Intercomparison and assessment of long-term (2004–2013) multiple satellite aerosol products over two contrasting sites in South Africa", J Atmos Sol Terr Phys **148** (2016) 82. http://dx.doi.org/10.1016/j.jastp.2016.09.001.

[46] B. N. Duncan, Y. Yoshida, B. De Foy, L. N. Lamsal, D. G. Streets, Z. Lu, K. E. Pickering & N. A. Krotkov, "The observed response of Ozone Monitoring Instrument (OMI) NO 2 columns to NO x emission controls on power plants in the United States : 2005 to 2011", Atmospheric Environment **81** (2013) 102. https://doi.org/10.1016/j.atmosenv.2013.08.068.

[47] B. N. Duncan, A. I. Prados, L. N. Lamsal, Y. Liu, D. G. Streets, P. Gupta, E. Hilsenrath, R. A. Kahn, J. E. Nielsen, A. J. Beyersdorf, S. P. Burton, A. M. Fiore, J. Fishman, D. K. Henze, C. A. Hostetler, N. A. Krotkov, P. Lee, M. Lin, S. Pawson, P. Gabriele, K. E. Pickering, R. B. Pierce, Y. Yoshida & L. D. Ziemba, "Satellite data of atmospheric pollution for U. S. air quality applications : Examples of applications, summary of data end-user resources, answers to FAQs, and common mistakes to avoid", Atmospheric Environment **94** (2014) 647. https://doi.org/10.1016/j.atmosenv.2014.05.061.

[48] B. Onoz & M. Bayazit, "The power of statistical tests for trend detection", Turkish Journal of Engineering and Environmental Sciences **27** (2003) 247. https://www.researchgate.net/publication/282061007_The_Power_of_Statistical_Tests_for_Trend_Detection.

[49] A. Longobardi & P. Villani, "Trend analysis of annual and seasonal rainfall time series in the Mediterranean area", Int. J. Climatol **30** (2009) 1538. https://doi.org/10.1002/joc.2001.

[50] Q. He, C. Li, F. Geng, Y. Lei & Y. Li, "Study on Long-term aerosol distribution over the Land of East China Using MODIS Data", Aerosol and Air Quality Research **12** (2012) 304. https://doi.org/10.4209/aaqr.2011.11.0200.

[51] T. F. Eck, B. N. Holben, A. Sinyuk, R. T. Pinker, P. Goloub, H. Chen, B. Chatenet, Z. Li, R. P. Singh, S. N. Tripathi, J. S. Reid, D. M. Giles, O. Dubovik, N. T. O. Neill, A. Smirnov, P. Wang & X. Xia, "Climatological aspects of the optical properties of fine / coarse mode aerosol mixtures", Journal of Geophysical Research **115** (2010) 1. https://doi.org/10.1029/2010JD014002.

[52] J. Lin, Y. Zheng, X. Shen, L. Xing & H. Che, "Global aerosol classification based on Aerosol Robotic Network (AERONET) and satellite observation", Remote Sens. **13** (2021) 1114. https://doi.org/10.3390/rs13061114.

[53] S. S. Aladodo, C. O. Akoshile & J. O. Otu, "A Review of evidence of aerosol transmission of SARS-CoV-2 particles", J. Nig. Soc. Phys. Sci. **3** (2021) 234. https://doi.org/10.46481/jnsps.2021.162.

[54] E. Jurado, F. M. Jaward & R. Simo, "Atmospheric dry deposition of persistent organic pollutants", Remote Sensing of Environment **38** (2004) 5505. https://doi.org/10.1021/es049240v.

[55] W. Slinn, "Predictions for particle deposition to vegetative canopies", Atmospheric Environment **16** (1988) 1785. https://doi.org/10.1016/0004-6981(82)90271-2.

[56] S.-W. Kim, P. Chazette, F. Dulac, J. Sanak, B. Johnson & S.-C. Yoon, "Transport and vertical structure of aerosols and water vapor over West Africa during the African monsoon dry season", Atmospheric Chemistry and Physics Discussions **9** (2009) 1831. https://doi.org/10.5194/acpd-9-1831-2009.

[57] I. Abubakar & O. I. Adesola, "Statistical and trend analyses of rainfall in Sokoto", International Research Journal of Engineering Science, Technology and Innovation (IRJESTI) **1** (2012) 161. https://www.interesjournals.org/articles/statistical-and-trend-analyses-of-rainfall-in-sokoto.pdf.

[58] J. Rajot, "AMMA dust experiment: An overview of measurements during the dry season special observation period (SOP0) at Banizoumbou (Niger) supersite", Journal of Geophysical Research **113** (2008) D23. https://doi.org/10.1029/2008JD009906.

[59] R. T. Pinker, H. Liu, S. R. Osborne & C. Akoshile, "Radiative effects of aerosols in Sub-Sahel Africa:Dust and Biomass burning", Journal of Geophysical Research Atmospheres **115** (2010) n/a. https://doi.org/10.1029/2009JD013335.

[60] I. N. Sokolik & O. B. Toon, "Direct radiative forcing by anthropogenic airborne mineral aerosol", Nature **381** (1996) 681. https://doi.org/10.1038/381681a0.

[61] P. B. Russell, R. W. Bergstrom, Y. Shinozuka, A. D. Clarke, P. F. Decarlo, J. L. Jimenez & J. M. Livingston, "Absorption angstrom exponent in AERONET and related data as an indicator of aerosol composition", **10** (2010) 1155. https://doi.org/10.5194/acp-10-1155-2010.

[62] S. S. Aladodo, C. O. Akoshile, T. B. Ajibola, O. A. Falaiye & M. Sani, "Monitoring and estimation of aerosol and air pollutants relations using multi-sensor satellite and ground remote sensing over Ilorin a sub-sahel", Monograph of Atmos. Res. **1** (2018) 24. https://carnasrda.com/wp-content/uploads/2019/06/Aladodo-et-al.pdf.

[63] R. J. Charlson, S. E. Schwartz, J. M. Hales, R. D. Cess, J. A. Coakley Jr., J. E. Hansen & D. J. Hofmann, "Climate forcing by anthropogenic aeroso", Science **255** (1992) 423. https://doi.org/10.1126/science.255.5043.423.